

Synthesis, Structure, and Ferromagnetism of a New Oxygen Defect Pyrochlore System $\text{Lu}_2\text{V}_2\text{O}_{7-x}$ ($x = 0.40\text{--}0.65$)

G. T. Knoke,* A. Niazi,[†] J. M. Hill, and D. C. Johnston

Ames Laboratory and Department of Physics and Astronomy, Iowa State University, Ames, Iowa 50011

(Dated: February 4, 2018)

A new fcc oxygen defect pyrochlore structure system $\text{Lu}_2\text{V}_2\text{O}_{7-x}$ with $x = 0.40\text{--}0.65$ was synthesized from the known fcc ferromagnetic semiconductor pyrochlore compound $\text{Lu}_2\text{V}_2\text{O}_7$ which can be written as $\text{Lu}_2\text{V}_2\text{O}_6\text{O}'$ with two inequivalent oxygen sites O and O'. Rietveld x-ray diffraction refinements showed significant Lu-V antisite disorder for $x \gtrsim 0.5$. The lattice parameter versus x (including $x = 0$) shows a distinct maximum at $x \sim 0.4$. We propose that these observations can be explained if the oxygen defects are on the O' sublattice of the structure. The magnetic susceptibility versus temperature exhibits Curie-Weiss behavior above 150 K for all x , with a Curie constant C that *increases* with x as expected in an ionic model. However, the magnetization measurements also show that the (ferromagnetic) Weiss temperature θ and the ferromagnetic ordering temperature T_C both strongly *decrease* with increasing x instead of increasing as expected from $C(x)$. The T_C decreases from 73 K for $x = 0$ to 21 K for $x = 0.65$. Furthermore, the saturation moment at a field of 5.5 T at 5 K is nearly independent of x , with the value expected for a fixed spin 1/2 per V. The latter three observations suggest that $\text{Lu}_2\text{V}_2\text{O}_{7-x}$ may contain localized spin 1/2 vanadium moments in a metallic background that is induced by oxygen defect doping, instead of being a semiconductor as suggested by the $C(x)$ dependence.

I. INTRODUCTION

The surprising discovery of heavy fermion behaviors in the metallic fcc normal spinel structure d -electron compound LiV_2O_4 at low temperatures $T \lesssim 10$ K (Refs. 1,2) illustrates that highly unconventional ground states can accrue to metallic compounds in which geometric frustration for antiferromagnetic ordering is present within a magnetic sublattice of the structure. At high $T \gtrsim 50$ K the V spin $S = 1/2$ sublattice interacts antiferromagnetically and consists of corner-sharing tetrahedra with the edges of the tetrahedra running along the six [110] crystal directions. Each V tetrahedron of course consists of triangles for which a collinear antiferromagnetic ordering does not minimize the interaction energy of the sublattice. This geometric frustration has a tendency to suppress static long-range antiferromagnetic ordering, and in the case of LiV_2O_4 probably contributes to the formation at low temperatures of a heavy fermion state instead.

In our search for the same or other novel ground states of such metallic oxide systems containing frustrated arrays of local magnetic moments, we turned to materials crystallizing in the well-known fcc pyrochlore structure³ with generic formula $\text{A}_2\text{B}_2\text{O}_7$ in which the interpenetrating A and B sublattices are each identical to the V sublattice in LiV_2O_4 .⁴ The pyrochlore structure has been very popular and important for the study of geometric magnetic frustration effects, but most such studies have been on insulating rather than metallic systems. There are two crystallographically inequivalent types of oxygen atoms O and O' in the structure, corresponding to the formula $\text{A}_2\text{B}_2\text{O}_6\text{O}'$, as illustrated in Fig. 1 for the known ferromagnetic semiconducting pyrochlore compound $\text{Lu}_2\text{V}_2\text{O}_7$ with a Curie temperature T_C of

about 73 K.^{5,6,7,8,9,10,11,12} This compound contains V^{+4} d^1 cations with spin $S = 1/2$ which give rise to the magnetic ordering (the Lu^{+3} cations are nonmagnetic). Interestingly, the O' atoms are located at the centers of the Lu^{+3} tetrahedra. The result of this is that the Lu site is eight-fold coordinated by oxygen as compared to the six-fold coordination of V. Thus in $\text{A}_2\text{B}_2\text{O}_7$ pyrochlore compounds the A atom is often a lanthanide atom and the B atom is often a transition metal. In the absence of the O' atoms, both the Lu and V atoms would have been 6-fold coordinated by oxygen; this is relevant to our proposed structural model for the oxygen defects in $\text{Lu}_2\text{V}_2\text{O}_{7-x}$ to be introduced later in Sec. II C.

In an attempt to dope the compound $\text{Lu}_2\text{V}_2\text{O}_7$ to induce metallic character, we tried to synthesize the unknown hypothetical compound $\text{Lu}_2\text{V}_2\text{O}_6\text{F}$ in which the O' atom in $\text{Lu}_2\text{V}_2\text{O}_7$ would be completely replaced by F, leading to a crystallographically ordered compound with a non-integral oxidation state of +3.5 for V as in LiV_2O_4 . If the structure remained cubic, that compound would have been metallic by symmetry. Using conventional solid state methods, a clean synthesis was carried out in a sealed Mo crucible at 1250 °C, but unfortunately the product did not crystallize in the pyrochlore structure.

In a further attempt to induce a non-integral V oxidation state in $\text{Lu}_2\text{V}_2\text{O}_7$, we next tried to create oxygen vacancies that would result in the composition $\text{Lu}_2\text{V}_2\text{O}_{7-x}$; for $x = 1/2$, the oxidation state of the V would again be +3.5 as in LiV_2O_4 . These efforts were successful as described herein, yielding compounds with $x = 0.40\text{--}0.65$. Our different types of magnetization data give conflicting indications regarding the metallic character of $\text{Lu}_2\text{V}_2\text{O}_{7-x}$, as will be described. In general, the crystallographic and magnetic properties evolve in interesting and unexpected ways with increasing x . Here we report

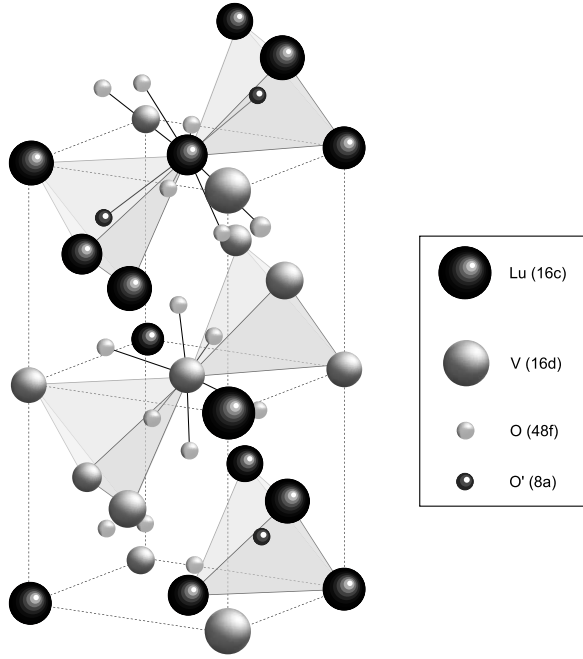


FIG. 1: Pyrochlore crystal structure of $\text{Lu}_2\text{V}_2\text{O}_7$.

the synthesis, structure, and magnetic properties of the new oxygen defect pyrochlore system $\text{Lu}_2\text{V}_2\text{O}_{7-x}$. The synthesis and structural studies are presented in Sec. II, and the magnetization measurements and analyses are in Sec. III. A summary is given in Sec. IV.

II. SYNTHESIS AND STRUCTURE OF $\text{Lu}_2\text{V}_2\text{O}_{7-x}$ ($x = 0, 0.40 - 0.65$)

A. Synthesis

$\text{Lu}_2\text{V}_2\text{O}_7$ was synthesized by calcining pelletized stoichiometric quantities of 99.995% pure (metals basis) Lu_2O_3 (Stanford Materials Corp.), V_2O_3 and V_2O_5 (MV Laboratories, Inc.) in sealed silica tubes at 1250 °C for 72 hours with two intermediate grindings. Samples of $\text{Lu}_2\text{V}_2\text{O}_{7-x}$ were subsequently prepared by reducing powdered $\text{Lu}_2\text{V}_2\text{O}_7$ in a mixture of 4.5% H_2 in He at temperatures ranging from 550 to 750 °C as listed in Table II below. If the reduction temperature was increased to 800 °C, x-ray and magnetization data showed that the different compound LuVO_3 (see, e.g., Refs. 13,14) was obtained instead of pyrochlore structure $\text{Lu}_2\text{V}_2\text{O}_{7-x}$. The most effective method of synthesis was to reduce a sample of $\text{Lu}_2\text{V}_2\text{O}_7$ under flowing H_2/He gas in a Perkin-Elmer Thermogravimetric Analyzer (TGA). Synthesis was regarded as complete when weight loss ceased at a given temperature and the weight remained stable for at least one hour. The time to completion depended on a combination of factors including the reduction temperature and the amount of sample used. Typical samples (40–50 mg) took approximately two days to stabilize

at a reduced composition, larger samples more than three days. The most homogeneous samples were produced by heating at a ramp rate of 2 °C/min followed by a two-day hold and a subsequent 2 °C/min cooling rate with a 15 min hold after room temperature had been reached to allow the TGA to stabilize. Two series of $\text{Lu}_2\text{V}_2\text{O}_{7-x}$ samples, “gtk-4-11-n” and “gtk-4-5c2-n”, were synthesized and studied.

The oxygen content of the parent $\text{Lu}_2\text{V}_2\text{O}_7$ samples was determined via oxidation to V^{+5} in the TGA under O_2 . A typical value of the oxygen content was 6.98(7). For the oxygen deficient $\text{Lu}_2\text{V}_2\text{O}_{7-x}$ samples, the weight loss during synthesis in the TGA was used to calculate the oxygen content, assuming the parent compound had exactly $x = 0$. Attempts to produce $\text{Lu}_2\text{V}_2\text{O}_{7-x}$ in a tube furnace under flowing H_2 in He were largely unsuccessful. The precise temperature of the sample within the furnace was difficult to measure and it was impossible to know when the reduction had ceased without a constant monitor on the weight. Checking the weight periodically by removing the sample from the furnace proved disastrous as repeated heating and cooling cycles caused the samples to decompose. These samples had multiple Curie temperatures, were generally of poor quality, and will not be further discussed. In view of these results and the relatively low temperatures (550–750 °C) at which the samples are synthesized compared to the temperature (1250 °C) needed to synthesize the $\text{Lu}_2\text{V}_2\text{O}_7$ parent compound, the oxygen defect system $\text{Lu}_2\text{V}_2\text{O}_{7-x}$ may be metastable.

B. Structure

Powder x-ray diffraction (XRD) patterns were obtained using a Rigaku Geigerflex diffractometer and $\text{Cu K}\alpha$ radiation, in the 2θ range from 5 to 110° with a 0.02° step size. Intensity data were accumulated for 5 to 10 s per step. The small powder sample amounts available ($\lesssim 50$ mg, see above) constrained us to mount the powder on vaseline-coated glass microscope slides for XRD specimens. The amorphous vaseline and glass background at low angles restricted subsequent Rietveld refinement of some of the XRD patterns to $2\theta > 20^\circ$. However, the restricted range eliminated only the initial (111) reflection and did not significantly affect the results. A typical sample of $\text{Lu}_2\text{V}_2\text{O}_{7-x}$ showed a single phase x-ray diffraction pattern with lattice parameters similar to those of the parent compound as shown for several samples in Fig. 2. It is important to note that the intensities of the reflections with Miller indices $(h k l)$ all odd become greatly suppressed with increasing oxygen deficiency above $x \approx 0.4$ compared to the reflections with $(h k l)$ all even. This reduction in the (odd, odd, odd) reflection intensities is a very sensitive indicator of antisite disorder between the Lu and V sites of the pyrochlore structure as reported for (Sc,Lu)-V antisite disorder in the system $(\text{Lu}_{1-x}\text{Sc}_x)_2\text{V}_2\text{O}_7$.⁹ This means that Lu and

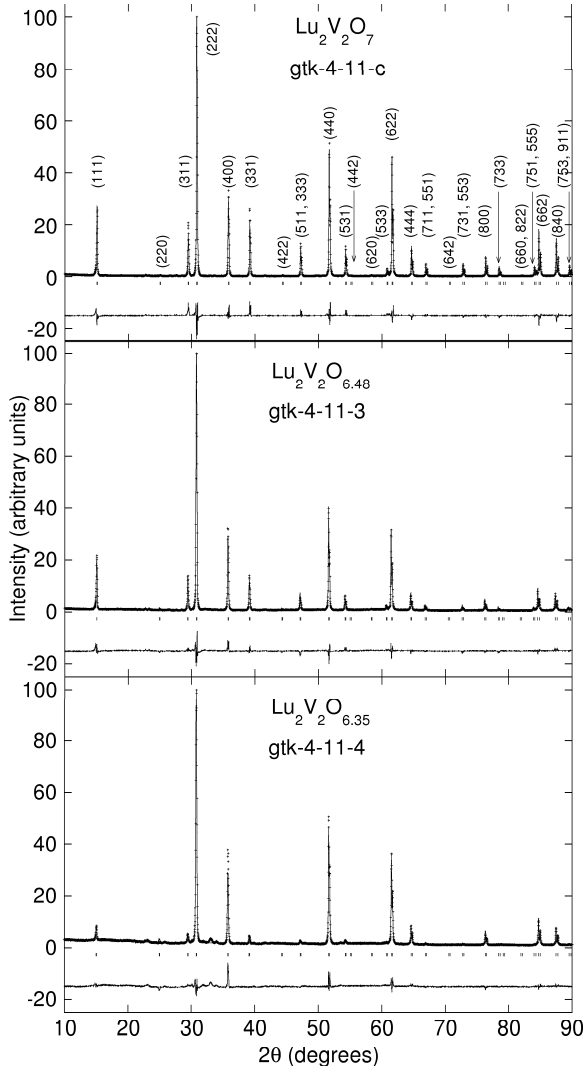


FIG. 2: Indexed X-ray powder diffraction patterns obtained using $\text{CuK}\alpha$ radiation, their Rietveld refinement fits, the expected line positions (ticks), and the differences between observed and calculated intensities, for three single-phase samples of $\text{Lu}_2\text{V}_2\text{O}_{7-x}$ with $x = 0.00, 0.52$, and 0.65 . The strong decrease in the (odd odd odd) reflection intensities with increasing x results from Lu-V antisite disorder. The goodnesses of fit were $R_{\text{wp}} = 15.0\%$ for $x = 0$, $R_{\text{wp}} = 12.3\%$ for $x = 0.52$, and $R_{\text{wp}} = 11.0\%$ for $x = 0.65$. The respective $R_{\text{wp}}/R_{\text{p}}$ values are given in Table II.

V atoms switch places to increasing degrees with increasing oxygen deficiency x .

To quantitatively characterize the changes in the structure of $\text{Lu}_2\text{V}_2\text{O}_{7-x}$ with increasing x , Rietveld refinements of the x-ray diffraction data were carried out using the program DBWS9807a.¹⁵ The atomic positions of the atoms in the pyrochlore structure of $\text{Lu}_2\text{V}_2\text{O}_7$ are shown in Table I, together with several parameters associated with the Rietveld refinements. Table I shows that the Lu, V, and O' positions are all fixed with respect to the unit cell edges, and only the z coordinate of the O position

TABLE I: Crystal data for $\text{Lu}_2\text{V}_2\text{O}_{7-x}$

Space Group	$Fd\bar{3}m$ (#227), origin at center ($\bar{3}m$)
Z	8
Atomic positions	Lu, 16(c), ($\bar{3}m$), (0,0,0) V, 16(d), ($\bar{3}m$), ($\frac{1}{2}, \frac{1}{2}, \frac{1}{2}$) O, 48(f), mm , ($\frac{1}{8}, \frac{1}{8}, z$) O', 8(a), $43m$, ($\frac{1}{8}, \frac{1}{8}, \frac{1}{8}$)
Wavelength	1.54060 Å
2θ range	5 – 110°
Number of reflections	90
Profile function	pseudo-Voigt

is variable. The initial O z -coordinate was taken to be that reported for $\text{Lu}_2\text{V}_2\text{O}_7$ by Soderholm and Greedan.¹² Keeping in mind the limitations of our XRD data, the TGA results were used to determine the oxygen site occupancy, with the vacancies being ascribed to the O' site (see the structural model in Sec. II C below). Thus we did not refine the oxygen site occupancies. Similarly, the quality of the XRD patterns was such that only an overall isotropic thermal parameter B was refined. Furthermore, the surface roughness was not refined, which can affect the fitted values of B . The parameters refined were B , scale, sample height, sample transparency, background, lattice spacing, the O position z value, pseudo-Voigt profile shape, full-width at half-maximum, and the Lu-V antisite disorder. The XRD patterns of samples with overall $x < 0.5$ showed the presence of stoichiometric $\text{Lu}_2\text{V}_2\text{O}_7$ (~ 20 mol% or less) in addition to $\text{Lu}_2\text{V}_2\text{O}_{7-x}$, probably due to kinetic limitations during the reduction process, and were refined as 2-phase mixtures. The reported structure parameters for $\text{Lu}_2\text{V}_2\text{O}_{7-x}$ are those refined for this phase. Bond lengths and angles were computed from the refined structure parameters using PowderCell for Windows.¹⁶ The XRD refinement parameters are shown in Table II. The Reitveld refinement fits for single phase samples with $x = 0, 0.52$ and 0.65 are shown in Fig. 2.

The lattice parameter and Lu-V antisite disorder are plotted as functions of the oxygen deficiency x for the two series of $\text{Lu}_2\text{V}_2\text{O}_{7-x}$ samples in Fig. 3(a). The lattice parameter varies nonmonotonically, initially increasing and then decreasing for increasing x , thus strongly violating Vegard's law. In the absence of samples with $0 < x < 0.4$ it is not possible to pinpoint the x value corresponding to the maximum in the lattice parameter, but similar behavior was observed for both series of samples. The refined Lu-V antisite disorder in Fig. 3(a) becomes significant for $x \gtrsim 0.5$ and then increases monotonically with increasing x . The lattice parameter decreases approximately linearly with the Lu-V antisite disorder for $x \geq 0.4$ as shown in Fig. 3(b).

TABLE II: Structure parameters for $\text{Lu}_2\text{V}_2\text{O}_{7-x}$ refined from powder XRD data. T_{prep} is the preparation temperature. The overall isotropic thermal parameter B is defined within the temperature factor of the intensity as $e^{-2B \sin^2 \theta / \lambda^2}$.

Sample	T_{prep} (° C)	x	a (Å)	z of O at 48(f)	Lu-V Disorder	V-O-V (°)	B (Å ²)	$R_{\text{wp}}/R_{\text{p}}$
gtk-4-			(Å)					
5-c2	1250	0	9.9368(1)	0.4258(5)	0 ^a	134.5	0.62(2)	1.30
5-c2-7 ^b	550	0.44	9.9721(3)	0.4155(9)	0.003(2)	128.9	2.47(4)	1.33
5-c2-5 ^b	650	0.52	9.9643(2)	0.4090(8)	0.052(2)	125.5	1.92(3)	1.32
5-c2-6	700	0.65	9.9502(3)	0.4067(6)	0.254(2)	124.4	2.79(3)	1.36
11-c	1250	0	9.9401(1)	0.4265(5)	0 ^a	134.8	1.03(2)	1.32
11-1 ^b	550	0.40	9.9618(2)	0.4190(9)	0.000(2)	130.6	2.94(4)	1.31
11-2 ^b	600	0.48	9.9604(3)	0.4141(8)	0.026(2)	128.1	3.12(4)	1.37
11-3	650	0.52	9.9560(2)	0.4114(6)	0.085(2)	126.7	3.12(3)	1.33
11-5	700	0.58	9.9526(3)	0.4057(7)	0.145(2)	123.8	2.73(3)	1.32
11-4	750	0.65	9.9424(3)	0.3912(8)	0.295(2)	116.9	2.72(3)	1.28

^aRietveld refinement of the XRD data gave small unphysical negative values (≈ -0.01) for the Lu-V antisite disorder, i.e., for site occupancy by the minority species [V at the Lu 16(c) site and Lu at the V 16(d) site]. The antisite disorder was therefore fixed to be zero for subsequent refinements.

^bTwo-phase sample with about 20 mol% or less (from Rietveld refinement of the XRD data) of stoichiometric $\text{Lu}_2\text{V}_2\text{O}_7$. The overall composition x and the refined fraction of the $\text{Lu}_2\text{V}_2\text{O}_{7-x}$ phase in each two-phase sample were 0.35 and 79(2)% for gtk-4-5-c2-7, 0.49 and 95(1)% for gtk-4-5-c2-5, 0.32 and 80(1)% for gtk-4-11-1, and 0.39 and 82(1)% for gtk-4-11-2. The composition and structure parameters reported in the table are for the oxygen defect $\text{Lu}_2\text{V}_2\text{O}_{7-x}$ phase in each sample.

C. Structural Model for Oxygen Vacancies in $\text{Lu}_2\text{V}_2\text{O}_{7-x}$

Typically, in oxides V^{+3} or V^{+4} cations are 6-fold coordinated by oxygen whereas the larger Lu^{+3} cation is often 8-fold coordinated, as in the pyrochlore structure of $\text{Lu}_2\text{V}_2\text{O}_7$ itself, although 6-fold coordination for Lu also occurs in some oxide compounds. In view of the Lu-V antisite disorder in $\text{Lu}_2\text{V}_2\text{O}_{7-x}$ that increases with increasing x , and of the nonmonotonic variation in the lattice parameter with x , we propose that the oxygen vacancies in $\text{Lu}_2\text{V}_2\text{O}_{7-x}$ occur on the O' sublattice of the structure, as follows. Since the O' anions reside at the centers of the Lu tetrahedra in $\text{Lu}_2\text{V}_2\text{O}_7$ as shown in Fig. 1, O' vacancies would decrease the average coordination number of the Lu sites by O, thus encouraging V atoms to occupy the Lu sites, which requires Lu to switch places with V (antisite disorder) in order to preserve the overall composition. If both of the O' atoms on either side of a given Lu site were vacant, which would occur with probability x^2 , that Lu site would then have 6-fold oxygen coordination as preferred by V cations. The antisite disorder in Fig. 3 is indeed seen to roughly follow an x^2 dependence.

In this model, we propose that the removal of oxygen from the O' sites at the centers of the Lu tetrahedra causes an initial increase in the lattice parameter with increasing x from $x = 0$ to $x = 0.32$ in Fig. 3(a). This

arises from the resultant removal of the Lu-O'-Lu bonding within the affected $\text{Lu}_4\text{O}'$ tetrahedra, thus causing the Lu_4 tetrahedra and the overall lattice to expand. However, at larger $x \gtrsim 0.4$, the smaller ionic radius of the Lu^{+3} ion in the 6-fold oxygen-coordinated V site, occurring via Lu-V antisite disorder, compared to its ionic radius in the original 8-fold coordinated Lu site, evidently leads to the observed lattice contraction. For $x = 0.40$ –0.65, the lattice parameter decreases approximately linearly by about 0.02 Å with increasing Lu-V antisite disorder as seen in Fig. 3(b). Indeed, this decrease is about the same as expected from the decrease in ionic radius of Lu^{+3} in 8-fold (0.977 Å) to 6-fold (0.861 Å) coordination by oxygen with increasing Lu-V antisite disorder, where one utilizes the facts that there are 16 Lu cations per unit cell and that the fractional Lu occupation of V sites increases from about 0 to 0.3 over this x range.

III. MAGNETIZATION MEASUREMENTS AND ANALYSES

Measurement Results

Magnetization M data were obtained at temperatures T between 1.8 and 300 K over the applied magnetic field H range from 0 to 5.5 T using a Quantum Design SQUID magnetometer. As shown for representative samples in

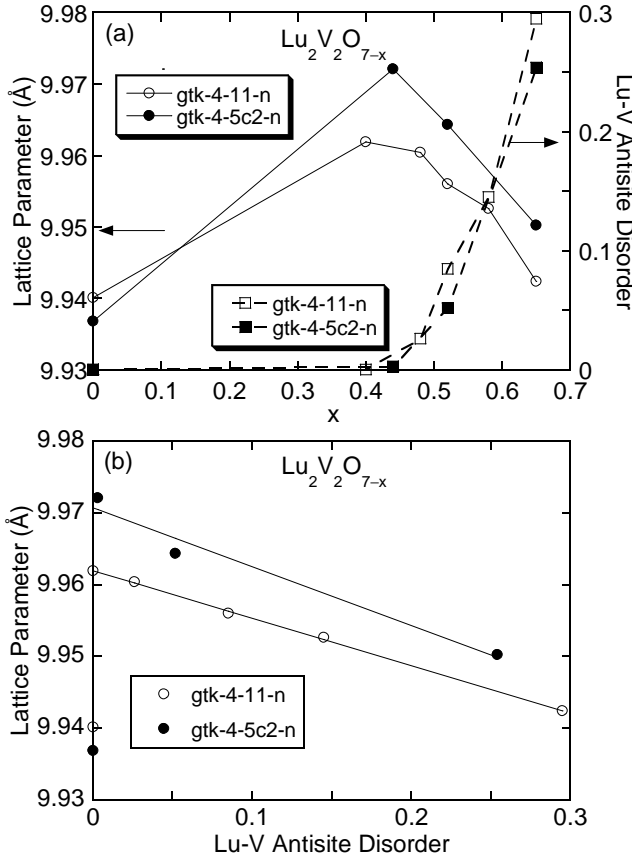


FIG. 3: (a) Refined lattice parameter (left scale) and Lu-V antisite disorder (right scale) as functions of x for two series of $\text{Lu}_2\text{V}_2\text{O}_{7-x}$ samples. (b) Refined lattice parameter as a function of the Lu-V antisite disorder. The straight lines are linear fits to the data for $x > 0.4$. The error bars are smaller than the size of the data symbols.

Fig. 4, the inverse susceptibility of each $\text{Lu}_2\text{V}_2\text{O}_{7-x}$ composition at temperatures above about 150 K follows the Curie-Weiss law $\chi = C/(T - \theta)$ with Curie constant C and Weiss temperature θ listed in Table III. Representative straight-line fits are shown in Fig. 4.

All $\text{Lu}_2\text{V}_2\text{O}_{7-x}$ samples ($x = 0.40\text{--}0.65$) exhibited ferromagnetic ordering. The Curie temperatures T_C (Table III) were determined from zero-field-cooled and field-cooled $M(T)$ measurements at a low field $H = 10\text{ G}$ or 20 G , shown in Fig 5(a) for a few of the samples. The straight line fit to the $M(T)$ data used to determine T_C is exemplified for the $x = 0.65$ sample in Fig 5(b). Isothermal magnetization $M(H)$ curves at $T = 5\text{ K}$ are plotted in Fig. 6. The samples with $x \gtrsim 0.5$, containing significant Lu-V antisite disorder, did not completely saturate up to at least $H = 5.5\text{ T}$. The well-defined saturation moments μ_{sat} for samples with $x < 0.5$ are listed in Table III. Assuming a spectroscopic splitting factor (“g-factor”) $g = 2$, the saturation moment of the $x = 0$ sample is close to the expected value $\mu_{\text{sat}} = gS\mu_{\text{B}} = 1\text{ }\mu_{\text{B}}/\text{V atom}$, since $S = 1/2$ for the V^{+4} cations in that compound. On the other hand, the magnetizations of all the

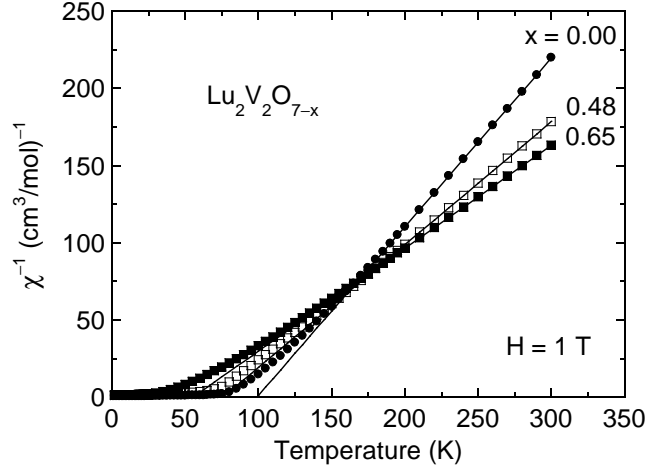


FIG. 4: Inverse of the magnetic susceptibility χ versus temperature in a magnetic field of 1 T for illustrative $\text{Lu}_2\text{V}_2\text{O}_{7-x}$ samples with $x = 0$, 0.48 , and 0.65 . The Curie-Weiss law fits above 150 K are shown as straight lines and are extrapolated to lower temperatures. The sample with (corrected) $x = 0.48$ contains 20(1)% of unreduced $\text{Lu}_2\text{V}_2\text{O}_7$ which has been corrected for in the plotted data.

other samples are also clustered around $1\text{ }\mu_{\text{B}}/\text{V atom}$ at our highest field of 5.5 T , contrary to expectation (below) that μ_{sat} should increase with increasing x .

The T_C , θ and C are plotted in Fig. 7(a) versus oxygen deficiency x in $\text{Lu}_2\text{V}_2\text{O}_{7-x}$, where for samples with $x < 0.5$ containing unreduced $\text{Lu}_2\text{V}_2\text{O}_7$, the Curie constants and Weiss temperatures have been corrected to reflect the values of the $\text{Lu}_2\text{V}_2\text{O}_{7-x}$ phase in those three samples. One sees that as the Curie constant C increases, both the Weiss temperature θ and the T_C decrease, contrary to expectation (see below). The θ for each sample is consistently $\sim 30\text{ K}$ higher than T_C , suggesting that T_C is suppressed from the mean-field value $T_C = \theta$ by fluctuation effects.

Magnetization Data Analysis

In the Curie-Weiss law $\chi = C/(T - \theta)$, the Curie constant C of a system of N spins S is expressed as

$$C = \frac{Ng^2S(S+1)\mu_{\text{B}}^2}{3k_{\text{B}}}, \quad (1)$$

where μ_{B} is the Bohr magneton and k_{B} is Boltzmann's constant. The Curie-Weiss law is a mean-field expression arising from only nearest-neighbor magnetic interactions and correlations between the spins in the system. For a system containing a random distribution of different spin values S , in mean field approximation one can replace $S(S+1)$ in Eq. (1) by its average value $\langle S(S+1) \rangle$, i.e.

$$C = \frac{Ng^2\langle S(S+1) \rangle\mu_{\text{B}}^2}{3k_{\text{B}}}. \quad (2)$$

TABLE III: Magnetic properties of $\text{Lu}_2\text{V}_2\text{O}_{7-x}$. Here, T_C is the Curie temperature; C the Curie constant and θ the Weiss temperature in the Curie-Weiss behavior of the high-temperature susceptibility; and $\mu_{\text{sat}}(5 \text{ K})$ the saturation moment at 5 K.

Sample	x	T_C (K)	C ($\text{cm}^3 \text{K/mol}$)	θ (K)	$\mu_{\text{sat}}(5 \text{ K})$ ($\mu_{\text{B}}/\text{V atom}$)
4-5-c2	0.00	73.8(1)	0.923(2)	97.4(3)	0.97
4-5-c2-7 ^a	0.44	39.0(4) ^a	1.31(2) ^a	72.0(3) ^a	0.95
4-5-c2-5 ^a	0.52	35.2(6) ^a	^b	^b	^c
4-5-c2-6	0.65	20.8(2)	^b	^b	^c
4-11-c	0.00	72.0(1)	0.825(1)	97.3(2)	0.95
4-11-1 ^a	0.40	37.1(4) ^a	1.20(1) ^a	79.8(5) ^a	0.99
4-11-2 ^a	0.48	36.1(12) ^a	1.37(1) ^a	71.5(5) ^a	0.93
4-11-3	0.52	32.2(1)	1.396(1)	66.9(2)	^c
4-11-5	0.58	27.9(1)	1.457(1)	62.6(1)	^c
4-11-4	0.65	20.3(2)	1.500(1)	55.4(1)	^c

^aThis sample shows a second ferromagnetic transition at 73 K indicating a significant fraction of the sample is $\text{Lu}_2\text{V}_2\text{O}_7$ (see Table II). The listed x is the corrected oxygen defect composition of the $\text{Lu}_2\text{V}_2\text{O}_{7-x}$ phase. Since the saturation moment does not significantly depend on the oxygen vacancy composition x in $\text{Lu}_2\text{V}_2\text{O}_{7-x}$, the mixture of $\text{Lu}_2\text{V}_2\text{O}_7$ with $\text{Lu}_2\text{V}_2\text{O}_{7-x}$ does not affect the value of the saturation moment. The observed C and θ values have been corrected so that the listed values correspond to the $\text{Lu}_2\text{V}_2\text{O}_{7-x}$ phase by itself. This was done by correcting the observed susceptibility for that of the relevant amount of the $x = 0$ phase and fitting the corrected data above 150 K by a Curie-Weiss law.

^bThe magnetic susceptibility at $H = 1 \text{ T}$ was not measured for this sample.

^cThe magnetization of this sample does not completely saturate up to an applied magnetic field $H = 5.5 \text{ T}$.

In $\text{Lu}_2\text{V}_2\text{O}_{7-x}$, the formal oxidation state of the V ions is $4 - x$. If the reduction in oxidation state with x does not give rise to itinerant electrons but rather to a random mixture of localized $S = 1/2$ (V^{+4}) and $S = 1$ (V^{+3}) spins, then in this ionic model the probabilities that $S = 1/2$ and $S = 1$ occur are $p_{1/2} = 1 - x$ and $p_1 = x$, respectively, yielding

$$\langle S(S+1) \rangle = \frac{3+5x}{4}. \quad (3)$$

If the g -factors of the spins $1/2$ and 1 are the same, one can substitute Eq. (3) into Eq. (2) to obtain the Curie constant as

$$C(x) = C(0) \left(1 + \frac{5x}{3}\right), \quad (4)$$

where for $g = 2$

$$C(0) = \frac{3}{4} \frac{\text{cm}^3 \text{K}}{\text{mol}}. \quad (5)$$

Here, a “mol” refers to a mole of $\text{Lu}_2\text{V}_2\text{O}_{7-x}$ formula units containing two moles of V atoms. The linear relation with no adjustable parameters in Eqs. (4) and (5) is

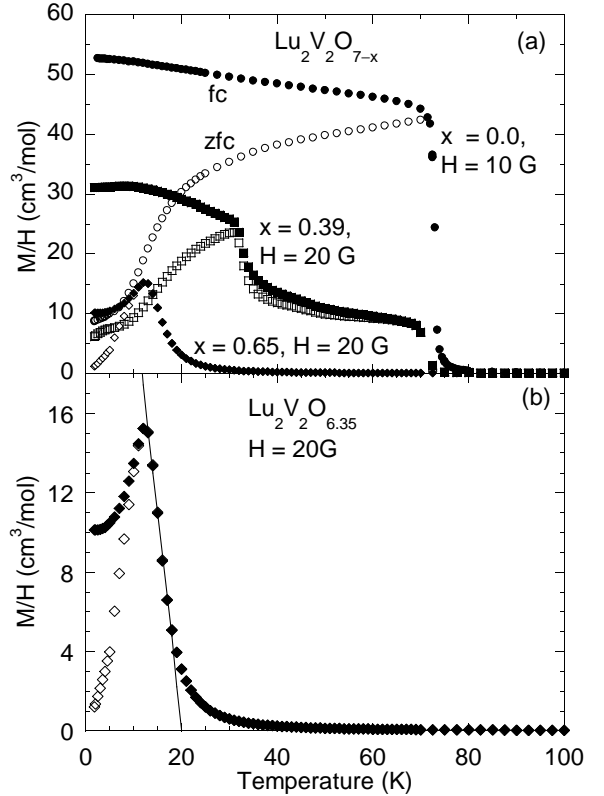


FIG. 5: (a) Zero-field-cooled (zfc, open symbols) and field-cooled (fc, filled symbols) magnetization versus temperature $M(T)$ data in low magnetic fields H for $x = 0.0, 0.39$, and 0.65 . The sample with overall $x = 0.39$ contained $18(2)\%$ of unreduced $\text{Lu}_2\text{V}_2\text{O}_7$, as seen in the corresponding $T_C \approx 73 \text{ K}$. (b) Expanded plots of the fc and zfc data for the $x = 0.65$ sample, showing the straight-line fit to the $M(T)$ data to determine the ferromagnetic ordering temperature T_C .

plotted as the straight line in Fig. 7(a), which describes well the Curie constant data for $x > 0$. This agreement suggests that increasing the oxygen vacancy concentration x results in the mixture of localized $S = 1/2$ and $S = 1$ V spin species dictated by the composition in an ionic model. This in turn suggests that the compound does not exhibit metallic character over our x range. However, one then expects that the saturation magnetic moment $\mu_{\text{sat}} = g\langle S \rangle \mu_{\text{B}} = (1+x)\mu_{\text{B}}$ at $H = 5.5 \text{ T}$ should increase with x , instead of remaining nearly independent of x as seen in Table III and Fig. 6.

For a uniform spin S system with the Heisenberg Hamiltonian $\mathcal{H} = -J \sum_{\langle ij \rangle} \vec{S}_i \cdot \vec{S}_j$ with nearest-neighbor exchange interaction J , where the sum is over nearest-neighbor spin pairs and $J > 0$ corresponds to ferromagnetic coupling, the mean-field ferromagnetic ordering (Curie) temperature is given by

$$T_C = \theta = \frac{zJS(S+1)}{3k_{\text{B}}}, \quad (6)$$

where z is the nearest-neighbor coordination number of a spin with neighboring spins. For a system containing

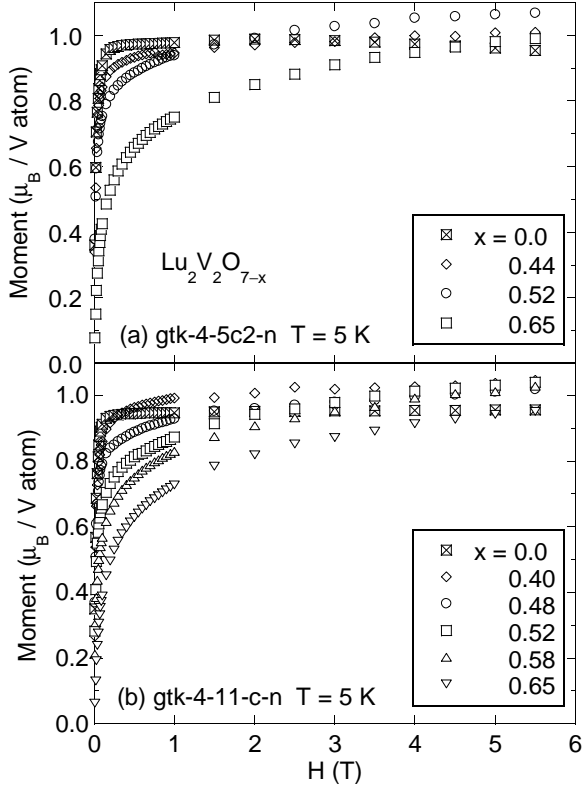


FIG. 6: Magnetization versus field at 5 K for the two series of $\text{Lu}_2\text{V}_2\text{O}_{7-x}$ samples (a) gtk-4-5-c2-n and (b) gtk-4-11-n. The samples with $x \gtrsim 0.5$ did not completely saturate up to at least 5.5 T. The samples with listed compositions $x = 0.44$ and 0.52 in (a), and $x = 0.40$ and 0.48 in (b), contain unreduced $\text{Lu}_2\text{V}_2\text{O}_7$ for which the listed compositions are the actual corrected x values in the oxygen defect phase $\text{Lu}_2\text{V}_2\text{O}_{7-x}$.

different spin values interacting with the same J for each nearest-neighbor spin pair, the Curie temperature at the mean field level is then

$$T_C = \frac{zJ\langle S(S+1) \rangle}{3k_B}. \quad (7)$$

Using Eqs. (2) and (7), one can eliminate $\langle S(S+1) \rangle$ and express T_C in terms of C as

$$T_C = \frac{zJC}{Ng^2\mu_B^2}. \quad (8)$$

Thus one expects that as the Curie constant increases with increasing x , T_C should also *increase*. Remarkably, we find instead from Table III and Fig. 7 that both θ and T_C *decrease* with increasing x .

From Eq. (8), one can express J in terms of T_C as

$$J = \frac{Ng^2\mu_B^2 T_C}{zC}. \quad (9)$$

Setting N to be twice Avogadro's number (there are two V atoms per formula unit in $\text{Lu}_2\text{V}_2\text{O}_{7-x}$), $g = 2$, $z = 6$

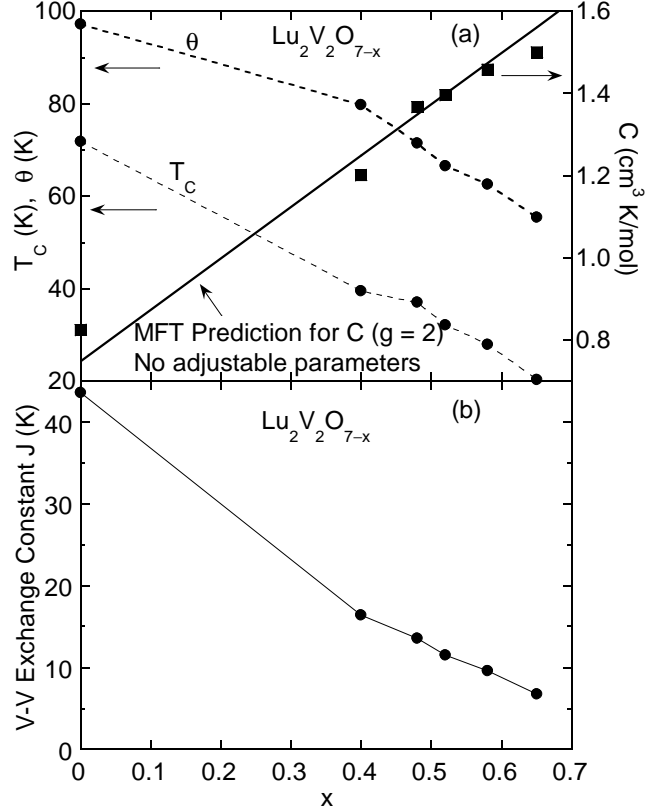


FIG. 7: (a) Curie temperature T_C , Weiss temperature θ (left scale) and Curie constant C (right scale) versus oxygen deficiency x in $\text{Lu}_2\text{V}_2\text{O}_{7-x}$ series gtk-4-11-n. The straight line is the mean field theory (MFT) prediction for C in Eqs. (4) and (5) assuming a spectroscopic splitting factor $g = 2$ for the local magnetic moments in the system, with no (other) adjustable parameters. (b) Variation of the exchange constant J versus composition x in $\text{Lu}_2\text{V}_2\text{O}_{7-x}$, computed using Eq. (10) and the C and T_C data in Table III.

from the structure, and taking C from Eqs. (4) and (5), Eq. (9) gives

$$J = 0.500 \frac{T_C}{C}, \quad (10)$$

where J and T_C are in units of K and C is in units of $\text{cm}^3 \text{K/mol}$. Using Eq. (10) and the $T_C(x)$ and $C(x)$ data in Table III, $J(x)$ was computed and is plotted in Fig. 7(b). One sees that J monotonically and strongly decreases with increasing x , by a remarkable factor of about 6 as x increases from 0 to 0.65.

IV. SUMMARY AND CONCLUSIONS

We have synthesized and studied the new defect pyrochlore series $\text{Lu}_2\text{V}_2\text{O}_{7-x}$ with $x = 0.40-0.65$ carried out in an attempt to dope the parent ($x = 0$) ferromagnetic semiconductor $\text{Lu}_2\text{V}_2\text{O}_7$ into the metallic state. The compound $\text{Lu}_2\text{V}_2\text{O}_7$ contains two crystallographically inequivalent oxygen sites denoted as O and O' sites,

and the composition can be written as $\text{Lu}_2\text{V}_2\text{O}_6\text{O}'$. For $x \gtrsim 0.5$, significant Lu-V antisite disorder clearly occurs that increases roughly as $\sim x^2$. This is consistent with our structural model for the oxygen vacancies, where oxygen depletion occurs at the O' site which is tetrahedrally coordinated by Lu in stoichiometric $\text{Lu}_2\text{V}_2\text{O}_6\text{O}'$. This model also appears to explain the anomalous nonmonotonic dependence of the lattice parameter on x which initially increases with x for $0 < x \lesssim 0.4$, and then decreases for $x \gtrsim 0.4$. We suggest that the $\text{Lu}_4\text{O}'$ tetrahedra (and the unit cell) first expand as O' atoms are removed from the centers of the Lu_4 tetrahedra, via elimination of the Lu- O' -Lu bonding within the affected Lu_4 tetrahedra, and then the unit cell subsequently shrinks with further increase in x due to the steadily reduced average oxygen coordination number of the Lu^{+3} cations. Our structural model for the oxygen vacancy position should be testable via future neutron diffraction studies of the O and O' site occupancies versus x in $\text{Lu}_2\text{V}_2\text{O}_{7-x}$ when samples of sufficient mass are synthesized.

Recent studies on Nb substitution effects, single crystal polarized neutron scattering measurements, and ^{51}V NMR studies indicate that a ferro-orbital ordered state accounts for the simultaneous ferromagnetic and semiconducting behaviour of the undoped $\text{Lu}_2\text{V}_2\text{O}_7$ parent compound.^{17,18,19} The oxygen defect pyrochlore series $\text{Lu}_2\text{V}_2\text{O}_{7-x}$ ($x = 0.40\text{--}0.65$) studied here remains ferromagnetic throughout. Unfortunately, the powder nature of the samples prevented us from carrying out conventional electronic transport measurements to determine whether the compounds are insulating or metallic (as $T \rightarrow 0$). The observed Curie constant C in the high-

temperature Curie-Weiss behavior of the magnetic susceptibility *increases* rapidly with increasing x , approximately following the mean field prediction for the mixture of localized $S = 1/2$ (V^{+4}) and $S = 1$ (V^{+3}) spins dictated by an ionic model for the composition x , suggesting the absence of metallic character of the material over our x range. However, the ferromagnetic ordering temperature T_C and Weiss temperature θ both strongly *decrease* monotonically with increasing x , which is opposite to the behaviors predicted from $C(x)$. Furthermore, the high-field (5.5 T) saturation moment at low temperatures (5 K) is nearly independent of x [$\mu_{\text{sat}} \approx 1 \mu_{\text{B}}/(\text{V atom})$], as expected for $S = 1/2$ and does not show the expected increase with increasing x , C and $\langle S \rangle$. These latter three anomalous behaviors suggest that the hole-doped $\text{Lu}_2\text{V}_2\text{O}_{7-x}$ series may actually be metallic, contrary to expectation from the observed $C(x)$, so that both localized ($S = 1/2$) and itinerant d -electrons may coexist. In that case one would need to explain why the conduction carriers give an apparent Curie-Weiss contribution to the magnetic susceptibility (in addition to that from the localized V^{+4} spins $1/2$) that increases with increasing x . These issues will be very interesting to examine further in future experimental and theoretical studies.

Acknowledgments

Ames Laboratory is operated for the U.S. Department of Energy by Iowa State University under Contract No. W-7405-Eng-82. This work was supported by the Director for Energy Research, Office of Basic Energy Sciences.

* Present address: Areté Associates, P.O. Box 6024, Sherman Oaks, California 91413

† Permanent address: Department of Physics, Faculty of Natural Sciences, Jamia Millia Islamia, New Delhi – 110025, India

¹ S. Kondo, D. C. Johnston, C. A. Swenson, F. Borsa, A. V. Mahajan, L. L. Miller, T. Gu, A. I. Goldman, M. B. Maple, D. A. Gajewski, E.J. Freeman, N. R. Dilley, R. P. Dickey, J. Merrin, K. Kojima, G. M. Luke, Y. J. Uemura, O. Chmaissem, and J. D. Jorgensen, Phys. Rev. Lett. **78**, 3729 (1997).

² For a concise review, see D. C. Johnston, Physica B **281&282**, 21 (2000).

³ M. A. Subramanian, G. Aravamudan, and G. V. Subba Rao, Prog. Solid State Chem. **15**, 55 (1983).

⁴ The A or B sublattice of the pyrochlore structure is itself often called “the pyrochlore structure” by physicists, a misnomer. The identical sublattice structure also occurs in the B sublattice of the cubic $\text{A}[\text{B}_2]\text{X}_4$ spinel structure and in the B sublattice of the AB_2 C-15 cubic Laves phase structure.

⁵ K. Kitayama and T. Katsura, Chem. Lett., 815 (1976).

⁶ G. Bazuev, D. Makarova, V. Oboldin, and G. Shveikin, Dokl. Akad. Nauk SSSR **230**, 869 (1976).

⁷ G. V. Bazuev, A. A. Samokhvalov, Yu. N. Morozov, I. I. Matveenko, V. S. Babushkin, T. I. Arbuzova, and G. P. Shveikin, Fiz. Tverd. Tela **19**, 3274 (1977).

⁸ T. Shin-ike, G. Adachi, and J. Shiokawa, Mater. Res. Bull. **12**, 1149 (1977).

⁹ J. E. Greedan, Mater. Res. Bull. **14**, 13 (1979).

¹⁰ L. Soderholm and J. E. Greedan, Mater. Res. Bull. **14**, 1449 (1979).

¹¹ L. Soderholm and J. E. Greedan, *Rare Earths in Modern Science and Technology* **2**, 393 (1980).

¹² L. Soderholm and J. E. Greedan, Mater. Res. Bull. **17**, 707 (1982).

¹³ H. C. Nguyen and J. B. Goodenough, Phys. Rev. B **52**, 324 (1995).

¹⁴ A. Muñoz, J. A. Alonso, M. T. Casais, M. J. Martínez-Lope, J. L. Martínez, and M. T. Fernández-Díaz, J. Magn. Magn. Mater. **272–276**, 2163 (2004).

¹⁵ Rietveld analysis program DBWS-9807a release 27.02.99, ©1998 by R. A. Young, an upgrade of “DBWS-9411 - an upgrade of the DBWS programs for Rietveld Refinement with PC and mainframe computers, R.A. Young, J. Appl. Cryst. **28**, 366 (1995)”.

¹⁶ Powder Cell for Windows, ver. 2.3, Dec 01, 1999, W. Kraus and G. Nolze.

¹⁷ S. Shamoto, N. Nakano, Y. Nozue, and T. Kajitani, *J. Phys. Chem. Solids* **63**, 1047 (2002).

¹⁸ H. Ichikawa, L. Kano, M. Saitoh, S. Miyahara, N. Furukawa, J. Akimitsu, T. Yokoo, T. Matsumura, M. Takeda, and K. Hirota, *J. Phys. Soc. Jpn.* **74**, 1020 (2005).

¹⁹ T. Kiyama, T. Shiraoka, M. Itoh, L. Kano, H. Ichikawa, and J. Akimitsu, *Phys. Rev. B* **73**, 184422 (2006).